

Electrochemical Properties of an Osmium (II) copolymer film and its electrocatalytic ability towards the oxidation of ascorbic acid in acidic and neutral pH

Kevin Foster and Timothy McCormac*

Centre for Research in Electroanalytical Technology "CREATE"

Department of Applied Science

Institute of Technology Tallaght (ITT) Dublin

Dublin 24

Ireland

Abstract

Copolymerisation of an Osmium (II) functionalised pyrrole moiety, Osmium -bis-N,N'-(2,2'-bipyridyl)-N-(pyridine-4-ylmethyl-(8-pyrrole-1-yl-octyl)-amine)chloride **(1)** with 3-methylthiophene was carried out. The resulting conducting polymer film exhibited a clear redox couple associated with the $\text{Os}^{3+/2+}$ response and the familiar conducting polymer backbone signature. The effect of film thickness upon the redox properties of the copolymer was investigated in organic electrolyte solutions. Scanning electron micrographs (SEM) along with energy dispersive X-ray (EDX) spectra of the copolymerised films were undertaken, both after formation and redox cycling in neutral buffer solution. These clearly show that electrolyte is incorporated into the polymer film upon redox cycling through the $\text{Os}^{3+/2+}$ redox system. The $\text{Os}^{3+/2+}$ response associated with the copolymer was seen to be significantly altered in the presence of ascorbic acid both in acidic and neutral pH buffer solutions. This pointed to an electrocatalytic reaction between the ascorbic acid and the Os^{3+} form of the copolymer. Under acidic conditions the copolymer film exhibited a sensitivity of 1.76 (\pm 0.05) $\mu\text{A} / \text{mM}$ with a limit of detection (LOD) of 1.45 μM for ascorbic acid. Under neutral pH conditions the copolymer exhibited a sensitivity of 19.26 (\pm 1.05) $\mu\text{A} / \text{mM}$ with a limit of detection (LOD) of 1.28 μM for ascorbic acid.

Keywords: Osmium, Pyrrole, Copolymerisation, 3-methylthiophene, ascorbic acid

**to whom correspondence should be addressed*

tim.mccormac@it-tallaght.ie Tel: +353-1-4042814; Fax: +353-1-4042700

1. Introduction

The selective amperometric determination of ascorbic acid (H_2A) is a major field of research primarily due to the various roles that it plays [1]. H_2A is electroactive and can be oxidised at positive potentials, the magnitudes of which depend upon the pH of the solution. However the kinetics of the oxidation are “sluggish” and the oxidation products tend to lead to electrode fouling [2]. Therefore modified electrode systems have been investigated for the selective amperometric determination of ascorbic acid both in acidic and neutral pH. Some of these systems include cyclodextrins [3], macrocyclic compounds [4, 5], conducting and redox polymeric films [2, 6-9], metalloporphyrins [10], polyoxometallates [11], transition metal hexacyanoferrates [12, 13] and ferrocene carboxylic acids [14, 15]. Previously [16] our group reported on the synthesis, characterisation, surface immobilisation and electrocatalytic properties of an Os(II) functionalised pyrrole monomer, namely, osmium-bis-*N,N'*-(2,2'-bipyridyl)-*N*-(pyridine-4-yl-methyl- (8-pyrrole-1-yl-octyl)-amine) chloride (**1**). Attempts to polymerise this pyrrole monomer proved unsuccessful probably due to the closeness of the bulky Os(II) bipyridyl moiety to the pyrrole ring. Our interest lies in the surface immobilisation of **1** through the employment of the well known copolymerisation technique. In terms of copolymerisation, the conducting polymer of choice has been polypyrrole [17, 18], this being primarily due to its “low oxidation potential” and “high conductivity” [19]. However recently thiophenes and its derivatives have been explored as possible matrixes for copolymerisation [20-22]. In this paper we report on the successful copolymerisation of **1** with 3-methylthiophene, electrochemical characterisation of the resulting films along with their electrocatalytic properties towards the oxidation of ascorbic acid. Our interest in an osmium polymer based system for the detection of ascorbic acid stems from previous work done on osmium based polymers for the determination of ascorbic acid [23], H_2O_2 [24], and glucose [25-27].

2.0 Experimental

2.1 Materials

1 was synthesised and characterised according to the literature [16]. All other chemicals were of reagent grade and used as received. Acetonitrile (HPLC grade water content 0.005%), was dried by storing over anhydrous calcium chloride for 24 hours and then over 4Å molecular sieves. The sieves having been activated in an oven at 523K overnight.

2.2 Apparatus and Procedures

Electrochemical experiments were performed in a single compartment three-electrode cell. The reference electrode employed, for the organic phase electrochemistry, was a silver wire in contact with an acetonitrile solution of AgNO₃ (0.01M) and 0.1M of the same supporting electrolyte as in the cell. For aqueous investigations a Ag/AgCl reference electrode, with 3M KCl, was employed. The working macroelectrode, namely a carbon (d = 2mm), was polished with 0.05 µm alumina, sonicated in deionised water for 5 mins, after which it was washed thoroughly with deionised water and acetone. The auxiliary electrode material was a platinum wire. A CH 660A potentiostat was employed for all electrochemical experiments. All organic solutions were prepared with dry HPLC grade acetonitrile with the aqueous buffers being prepared as detailed previously [16]. All electrolyte solutions were degassed with argon for 15 minutes prior to the electrochemical investigations at room temperature. Copolymer films of **1** and 3-methylthiophene were electrochemically deposited from acetonitrile solutions of 5mM **1** and 52mM 3-methylthiophene (3-MTHP) in 0.1M TEAP by cyclic voltammetry with a potential window of -0.1V to +1.4V, at a scan rate of 100 mV s⁻¹. This ratio between **1** and the **3-MTHP** was found to be ideal. Previous experiments were attempted with a range of 1:3MTHP ratios being employed (i.e.: 5mM:5mM; 2.5mM:10mM; 3mM:20mM; 3mM:30mM; 5mM:40mM; 5mM:10mM). However it was found that these films all exhibited either poor stability or low redox loadings of the Os²⁺ centre. After formation, each film was rinsed with the solvent-electrolyte system that its electrochemical behaviour was going to be investigated in. Scanning electron microscopy (SEM) was performed using a Hitachi S-2400N system. For SEM investigations, films were formed on 3 mm radius carbon disks.

3.0 Results and discussion

3.1 Electrochemical Characterisation of Copolymer Films

Previously our group has reported on the electrochemical characterisation of **1** [16]. As reported, **1** consists of a reversible redox couple associated with $\text{Os}^{3+/2+}$ system along with an irreversible pyrrole oxidation wave. Our previous attempts to polymerise **1** proved unsuccessful. As a result, in this article, the technique of copolymerisation of **1** with 3-methylthiophene has been undertaken. The formation of these copolymer films is described in the experimental section of the paper. Figure 1(a) illustrates the cyclic voltammogram obtained during the deposition of the copolymer. What is clearly seen is that upon continuous cycling there is a continual growth in peak currents associated with the $\text{Os}^{3+/2+}$ redox couple. Also what is apparent is the appearance of the redox signature associated with the polythiophene backbone at around +0.4V. Figure 1(b) illustrates the cyclic voltammogram obtained for the resulting copolymer film in blank 0.1 M tetraethyl ammonium perchlorate (TEAP) acetonitrile solution. What is clearly seen is the redox activity associated with the $\text{Os}^{3+/2+}$ couple with an $E_{1/2}$ of +0.09V (vs Ag/AgCl) along with the characteristic conducting polymer backbone electrochemical signature.

Investigations into the electrochemical behaviour of the copolymerised films of **1** were undertaken with the effect of film thickness being investigated. Table 1 summarises the variation in peak splitting and anodic and cathodic peak full widths at half maximum “*fwhm*” with sweep rate for a range of copolymers of varying surface coverages. Although the expected zero peak to peak separation and a *fwhm* of 90.6mV for a one electron process are not seen the typical trend of peak splitting and *fwhm* increasing with increasing scan rate are seen throughout for each film. The stability of the copolymer films of varying thicknesses towards redox cycling in 0.1M TEAP MeCN was investigated. It was found that all films were extremely stable to redox cycling through the $\text{Os}^{3+/2+}$ redox process as there was no reduction in the films electroactivities after 50 cycles. Plots of current vs. scan rate indicated thin film behaviour for films ($\Gamma = 1.3 \times 10^{-9} \text{ mol cm}^{-2}$) up to scan rates of approximately 250 mV s^{-1} . Such behaviour is expected for a surface-immobilised electroactive film which is thin enough to ensure that all redox active sites within the film undergo complete oxidation and reduction

during the potential cycle. For thicker films however ($\Gamma = 1.5 \times 10^{-8} \text{ mol cm}^{-2}$) linear relationships were only obtained up to scan rates of 80 mV s^{-1} , with an increase in peak splitting and a loss of peak symmetry at a specified scan rate.

Preliminary scanning electron micrographs (SEM) along with energy dispersive X-ray (EDX) images were taken of the copolymerised films both after formation and redox cycling through the $\text{Os}^{3+/2+}$ system in pH 7 buffer solution. Figures 2(a) and 2(b) illustrate the SEM images obtained of a copolymerised film after formation, at different magnifications. What is clearly seen is that the polymer surface appears to be not smooth in nature but more granular in nature with particles of roughly a few microns in diameter. The corresponding EDX images show the presence of the elements K, Cl, S, C, O and Os, as expected. Figures 2(c-e) represent the resulting SEM images of the film once it has been cycled through the $\text{Os}^{3+/2+}$ redox system in pH 7 buffer. What is clear is that the film has undergone structural modification. The film now appears to possess a dendritic type structure as well as the granular nature, also in figure 2(d) and more specifically in 2(e) crystals of KCl, from the buffer, are readily observed within the polymeric matrix. This is backed up by the EDX images of the film after cycling. This shows an increased response for K as well as a response for Na, thereby clearly indicating that the electrolyte is incorporated into the film upon redox cycling.

3.2 Electro catalytic activity of films towards ascorbic acid

Acidic Conditions

Figure 3(a) illustrates the irreversible oxidation of a 5mM ascorbic acid at a bare carbon electrode in pH 1.2, $E_{p,a}$ is +0.667V (vs. Ag/AgCl). In addition to the positive position of the anodic wave, it is well known that the products of ascorbic acid oxidation at a bare electrode cause fouling of the electrode's surface. Figure 3(b) illustrates the cyclic voltammogram obtained for an Os^{2+} copolymerised film, surface coverage $1.5 \times 10^{-8} \text{ mol cm}^{-2}$, in pH 1.2 buffer solution. What is again apparent is the reversible one electron couple associated with the $\text{Os}^{3+/2+}$ redox process. The film's stability towards redox cycling in this buffer medium was investigated and the film was found to be extremely stable, as seen in organic electrolyte

media. The film was then interacted with 5mM ascorbic acid and the resulting cyclic voltammogram is shown in figure 3(c). What is clearly seen is the significant change in the redox behaviour of the film with the ascorbic acid being oxidised by the Os^{3+} form of the coordinated metal centre in the copolymer. The catalytic wave associated with this interaction is situated at a less positive potential, namely $E_{p,a} = +0.45 \text{ V}$, as compared to that of the bare electrode in figure 3(a). It was found that upon increasing the ascorbic acid concentration there was an increase in the catalytic wave associated with the mediation process in conjunction with a decrease in the Os^{3+} reduction wave. Figure 3(d) shows how the catalytic current increases with increasing ascorbic acid concentration. It can be seen that the relationship is linear up to an approximate concentration of 8mM after which the response levels off. This is probably due to either the low availability of Os^{3+} sites which can effectively catalyse the oxidation of the higher concentrations of ascorbic acid.

The effect of surface coverage upon the magnitude of the catalytic current was investigated. It was found that for the interaction of 2mM ascorbic acid in pH 1.2 buffer, the magnitude of the I_{CAT} was 5.9, 1.1 and 0.6 μA for films of surface coverage, Γ , 9.1, 1.2 and 0.5 $\times 10^{-9} \text{ mol cm}^{-2}$, respectively. The effect of scan rate upon the interaction between ascorbic acid and the Os^{2+} copolymer was investigated. From comparing the two curves of $I_{p,a} v^{1/2}$ vs. $v^{1/2}$ in the absence and presence of ascorbic acid, it was found that the catalytic affect is apparent up to a scan rate of approximately 40mV s^{-1} . The operation of the Os^{2+} copolymer modified electrode as an amperometric sensor was investigated. An E_{app} of +0.45V was applied to the copolymer modified electrode under hydrodynamic conditions for approximately 20 minutes prior to the injection of the first addition of the ascorbic acid. The standard calibration curve obtained from performing the three separate I-t transients responses for the copolymerised films of similar surface converges (4.5 – 5.5 $\times 10^{-9} \text{ mol cm}^{-2}$) (n=3) is shown in Fig 2(e). It shows good linearity from 0.1 to 1.5 $\times 10^{-3}$ M of ascorbic acid with a correlation coefficient of 0.997, and a sensitivity of 1.76 (± 0.05) $\mu\text{A} / \text{mM}$. The limit of detection (LOD) for our system in acidic pH, based on three times the S/N ratio, was found to be 1.45 μM . In addition a response time of approximately 18-20 seconds was found in the initial stages of the calibration curve. I-t transients for the interaction of ascorbic acid with the polymer were

performed for films of varying thicknesses, 1×10^{-8} , 5.4×10^{-9} and 1.3×10^{-9} mol cm⁻². Standard calibration curves from the resulting I-t curves produced linear plots from approximately 0.1 to 1.5 mM with sensitivities of $3.4(\pm 0.04)$, $2.3(\pm 0.05)$ and $0.77(\pm 0.009)$ uA/mM for the films respectively. Thus clearly showing that the thicker film possessed the highest sensitivity, probably due to the higher number of electrocatalytic Os³⁺ sites within the film.

Investigations into the possible electrocatalytic ability of the poly (3-methylthiophene) backbone towards ascorbic acid was also investigated. A poly (3-methylthiophene) film was electrochemically deposited, from blank electrolyte (0.1M TEAP), by potential cycling between -0.2 and +1.4V. The film was then stabilised in pH 1.2 buffer and various additions of ascorbic acid were then added to the buffer medium. It was found that for 1mM ascorbic acid a irreversible peak at +0.65V was obtained, this is illustrated in figure 3(f). As the concentration of ascorbic acid is increased the position of this peak moves to more positive potentials. The positive nature of this peak clearly shows that the response obtained in figure 3(c) is due to the interaction between the Os³⁺ sites and the ascorbic acid.

Neutral conditions

As detailed in the previous section there is an electrocatalytic reaction between the Os³⁺ form of the copolymer and ascorbic acid in acidic conditions. This section details the preliminary work carried out into the electrocatalytic behaviour of the films towards ascorbic acid in neutral pH conditions. Figure 4(a) illustrates the irreversible oxidation of a 1mM ascorbic acid at a bare carbon electrode in pH 7.2, E_{p,a} is +0.221V. Figures 4(b) and (c) show the redox behaviour of the Os²⁺ copolymer, $\Gamma = 3 \times 10^{-9}$ mol cm⁻², in pH 7.2 buffer and the interaction between the film and 1mM ascorbic acid in pH 7.2, respectively. What is clear is that there is a similar reaction between the ascorbic acid and the Os³⁺ centre within the copolymer as detailed in the previous section. However the potential for this process is slightly more positive than the bare electrode reaction for ascorbic acid in neutral pH. However the advantages of our copolymer is that the observed catalytic current is significantly higher than at the bare electrode and that electrode fouling is avoided. The effect of ascorbic acid

concentration upon the measured catalytic current was investigated. A linear plot of I_{CAT} vs. [AA] was recorded up to an ascorbic acid concentration of approximately 25mM.

As discussed for the acidic medium, the response of the modified electrode to injections of ascorbic under hydrodynamic conditions was also performed. The standard calibration curve obtained from performing the three separate I-t transients responses for three separate polymer films ($n=3$) of similar surface converges ($4.5 - 6.6 \times 10^{-9} \text{ mol cm}^{-2}$) is shown in Fig 4(d). It shows good linearity from 0.1 to $1.5 \times 10^{-3} \text{ M}$ of ascorbic acid with a correlation coefficient of 0.999, and a sensitivity of $19.56 (\pm 1.05) \text{ uA / mM}$. The limit of detection (LOD) was found to be $1.28 \text{ }\mu\text{M}$, with response times of typically 18-20 seconds in the initial stages of the calibration curve.

Role of Possible Interferents

Previously, Lupu *et al* [28], investigated the effect of possible intereferents, on the behaviour of their “polythiophene derivative conducting polymer modified electrode” towards the electrocatalytic oxidation of ascorbic acid. Employing Lupu *et al*'s work as a basis for an investigation, we have conducted preliminary investigations into the effect of the presence of uric acid, acetaminophenol and glucose on the redox behaviour of our copolymerised conducting polymer films. . Figure 5(a) illustrates the cyclic voltammogram obtained when a Os^{2+} copolymerised film is interacted with 1mM glucose, in pH 7 buffer solution. What is clearly observed is that there is no change in the redox behaviour of the $\text{Os}^{3+/2+}$ redox system in the presence of the glucose. Increasing the glucose concentration to 5mM again showed no marked change in the polymers' redox activity. The effect of paracetamol addition on the redox behaviour of our copolymerised film was also investigated in buffer pH 7 solution. At the bare carbon electrode an oxidation wave ($E_{\text{p,a}}, +0.44\text{V}$) for the oxidation of 1mM paracetamol is observed with an associated current of $6.4\mu\text{A}$. Upon the addition of 1mM paracetamol to a carbon electrode modified with a copolymerised film of 1 with Γ of $4.8 \times 10^{-9} \text{ mol cm}^{-2}$, in pH 7 solution, there is a marked effect on the redox activity of the polymer film. The peak associated with the Os^{2+} centre moves from $+0.37\text{V}$ to $+0.48\text{V}$ with a large increase in current from 3.2 to $10.0\mu\text{A}$, but there is only a small increase in the peak current

associated with the Os^{3+} reduction wave with no change in peak potential. One possible explanation for this is that the paracetamol is able to diffuse freely through the polymer matrix and react at the underlying electrode. As a result the employment of this modified electrode towards the determination of paracetamol is not possible. Lupu *et al* also found that their polythiophene modified electrode was incapable of the determination of paracetamol. The response of the copolymerised film towards the oxidation of uric acid has also been investigated. It was found that the addition of 1mM uric acid caused an increase in the Os^{2+} oxidation wave in a very similar fashion to that observed with the ascorbic acid addition. Currently our group are trying to determine a strategy to separate out the two responses from both ascorbic and uric acid in pH 7 buffer for our polymer modified electrode system. These results observed are in good agreement with the work of Lupu *et al* [28].

4.0 Conclusion

There are several conclusions from our work

1. Extremely stable conducting polymer films have been obtained through copolymerisation of 3-methylthiophene and **1**, which exhibit a clear redox couple associated with an $\text{Os}^{3+/2+}$ system
2. The resulting copolymerised films exhibited a clear electrocatalytic effect upon the oxidation of ascorbic acid under acidic and neutral conditions.
3. Under acidic conditions the copolymer film exhibited a sensitivity of 1.76 (± 0.05) $\mu\text{A}/\text{mMol}$ with a limit of detection (LOD) of 1.45 μM for ascorbic acid.
4. Under neutral conditions the copolymer film exhibited a sensitivity of 19.26 (± 1.05) $\mu\text{A} / \text{mMol}$ with a limit of detection (LOD) of 1.28 μM for ascorbic acid.

Acknowledgements

Financial support obtained through the Irish Postgraduate Research and Development of Skills Programme through the grant TA 08 2002 and the ITT Dublin's 2005 PhD continuance fund is acknowledged. The authors would also like to thank Dr Aine Allen from ITT Dublin for the running of the SEM and EDX spectra of the polymer films.

References.

- [1] G. A. Gilman, W.T. Rall, A.S. Nies, P. Taylor, Goodman and Gilman's *The Pharmacological Basis of Therapeutics*, McGraw-Hill, Singapore, **1991**, 1547.
- [2] M. E. G. Lyons, W. Breen, J. Cassidy, *J. Chem. Soc. Faraday Trans.* **1991**, 87, 115.
- [3] M. I. Manzanares, V. Solis, R. H. de Rossi, *J. Electroanal. Chem.* **1997**, 430, 163.
- [4] V. S. Ijeri, P. V. Jaiswal, A. K. Srivastava, *Anal. Chimica. Acta.* **2001**, 439, 291.
- [5] J. Ren, H. Zhang, Q. Ren, C. Ren, C. Xia, J. Wan, Z. Qin, *J. Electroanal. Chem.* **2001**, 504, 59.
- [6] L. Zhang, S. Dong, *J. Electroanal. Chem.* **2004**, 568, 189.
- [7] J-B. Raoof, R. Ojani, S. Rashid-Nadimi, *Electrochimica. Acta.* **2004**, 49, 271.
- [8] A. P. Doherty, M. A. Stanley, J. G. Vos, *Analyst*, **1995**, 120, 2371.
- [9] G. Che, S. Dong, *Electrochimica Acta.* **1996**, 41, 381.
- [10] S-M. Chen, Y-L. Chen, *J. Electroanal. Chem.* **2004**, 573, 277.
- [11] C. Sun, J. Zhang, *Electrochimica. Acta.* **1998**, 43, 943.
- [12] C-X. Cai, K-H. Xue, S-H. Xu, *J. Electroanal. Chem.* **2000**, 486, 111.
- [13] M. H. Pournaghi-Azar, H. Razmi-Nerbin, *J. Electroanal. Chem.* **2000**, 488, 17.
- [14] L. Fernández, H. Carrero, *Electrochimica. Acta.* **2005**, 50, 1233.
- [15] J-B. Raoof, R. Ojani, A. Kiani, *J. Electroanal. Chem.* **2001**, 515, 45.
- [16] K. Foster, A. Allen, T. McCormac, *J. Electroanal. Chem.* **2004**, 573, 203.
- [17] B. Sari, M. Talu, *Synthetic Metals*, **1998**, 94, 221
- [18] K. Habermuller, A. Ramanavicius, V. Laurinavicius, W. Schuhmann, *Electroanalysis*, **2000**, 12, 1383
- [19] T. A. Scothorn, *Handbook of Conducting polymers*, 1st edition, Marcel Dekker, New York 1983
- [20] H. P. Welzel, G. Kossmehl, G. Engelmann, W. D. Hunnius, W. Plieth, *Electrochimica Acta.* **1999**, 44, 1827.
- [21] J. Ochmanska, P. G. Pickup, *J. Electroanal. Chem.* **1991**, 297, 197.
- [22] J. Roncali, *Chem. Rev.* **1992**, 92, 711.
- [23] A. P. Doherty, M. A. Stanley, J. G. Vos, *Analyst*, 1995, 120, 2371.

- [24] M. Dequaire, A. Heller, *Anal. Chem.* **2002**, 74, 4370.
- [25] L. Yang, E. Janle, T.H. Huang, J. Gitzen, P.T. Kissenger, M. Vreeke, A. Heller, *Anal. Chem.* **1995**, 67, 1326.
- [26] E. Csoregi, D.W. Schmidtke, A. Heller, *Anal. Chem.* **1995**, 67, 1240.
- [27] T.J. O_Hara, R. Rajagopalan, A. Heller, *Anal. Chem.* **1993**, 65, 3512.
- [28] S. Lupu, A. Mucci, L. Pigani, R. Seeber, C. Zanardi, *Electroanalysis*. **2002**, 14, No. 7-8, 519.

Figure Legends

Figure 1 (a) Repetitive cyclic voltammogram of 0.1mMol TEAP MeCN solution of 52:5mM of 3-methylthiophene:1 at a bare carbon electrode ($A=0.0314\text{cm}^2$). Scan rate = 100 mV s^{-1}

Figure 1 (b) Cyclic voltammogram of the copolymerised film from fig 1(a) in 0.1M TEAP MeCN on the carbon electrode ($A = 0.0314\text{ cm}^2$). Scan rate = 30 mV s^{-1}

Figures 2(a –b) SEM images of an immobilised copolymerised film deposited onto a carbon electrode ($A=0.0707\text{ cm}^2$) immediately after formation and drying.

Figures 2(c-e) SEM images of the copolymerised film from figure 2(a) after it has been electrochemically cycled through the $\text{Os}^{3+/2+}$ redox system in pH 7 buffer solution.

Figure 3(a) Cyclic voltammogram of 5mM ascorbic acid in pH 1.2 buffer at a bare carbon electrode ($A = 0.0314\text{ cm}^2$). Scan rate = 5 mV s^{-1}

Figure 3(b) Cyclic voltammogram of a copolymerised film of surface coverage $1.5 \times 10^{-8}\text{ mol cm}^{-2}$, on a carbon electrode ($A = 0.0314\text{ cm}^2$) in the aqueous pH 1.2 buffer solution. Scan rate = 5 mV s^{-1}

Figure 3(c) Cyclic voltammogram of the copolymerised film from fig 2(b) in pH 1.2 buffer in the presence of 5mM ascorbic acid. Scan rate = 5 mV s^{-1}

Figure 3(d) Plot of I_{CAT} versus [ascorbic acid] for the film in fig 2(c) in pH 1.2 buffer.

Figure 3(e) Standard calibration plot representing amperometric data ($n=3$) for the copolymerised film of **1** over the range of 0.1 – 1.5mM ascorbic acid in pH 1.2 buffer.

Figure 3(f) Cyclic voltammogram of poly (3-methylthiophene) film in pH 1.2 buffer in the absence (—) and presence (—) of presence of 1mM ascorbic acid. Scan rate = 5 mV s⁻¹

Figure 4(a) Cyclic voltammogram of 5mM ascorbic acid in pH 7.2 buffer at a bare carbon electrode (A = 0.0314 cm²). Scan rate = 5 mV s⁻¹

Figure 4(b) Cyclic voltammogram of a copolymerised film of surface coverage 3x10⁻⁹ mol cm⁻², on a carbon electrode (A = 0.0314 cm²) in the aqueous pH 7.2 buffer solution. Scan rate = 5 mV s⁻¹

Figure 4(c) Cyclic voltammogram of the copolymerised film from fig 4(b) in pH 7.2 buffer in the presence of 5mM ascorbic acid. Scan rate = 5 mV s⁻¹

Figure 4(d) Standard calibration plot representing amperometric data (n=3) for the copolymerised film of **1** over the range of 0.1 – 1.5mM ascorbic acid in pH neutral conditions.

Figure 5 Cyclic voltammogram of a copolymerised film of **1** on a carbon electrode (A = 0.0314 cm²) in the aqueous pH 7.2 buffer solution, in the absence (—) and presence (—) of 1mM glucose. Scan rate = 5mV s⁻¹

Table 1: Electrochemical parameters of copolymerised films of **1** with 3-methylthiophene formed by CV

Surface Coverage Γ (mol cm ⁻²)	Scan Rate mV s ⁻¹	Peak Splitting mV	Anodic peak fwhm mV	Cathodic peak fwhm mV
1.49 x 10 ⁻⁹	10	31	148	122
	40	48	136	116
	100	54	136	118
	400	58	124	124
6.25 x 10 ⁻⁹	10	34	152	106
	40	58	150	126
	100	85	160	132
	400	148	206	160
8.01 x 10 ⁻⁹	10	28	158	98
	40	46	154	115
	100	76	156	156
	400	133	178	168
4.07 x 10 ⁻⁸	10	36	212	118
	40	67	174	120
	100	118	182	120
	400	235	238	127

Figure 1 (a)

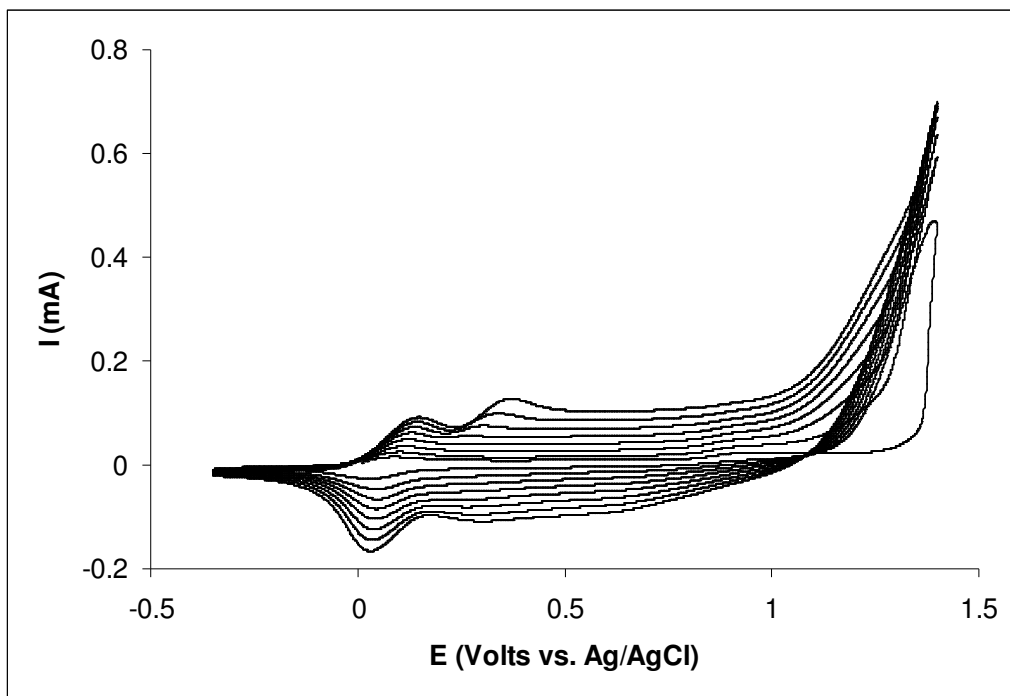


Figure 1 (b)

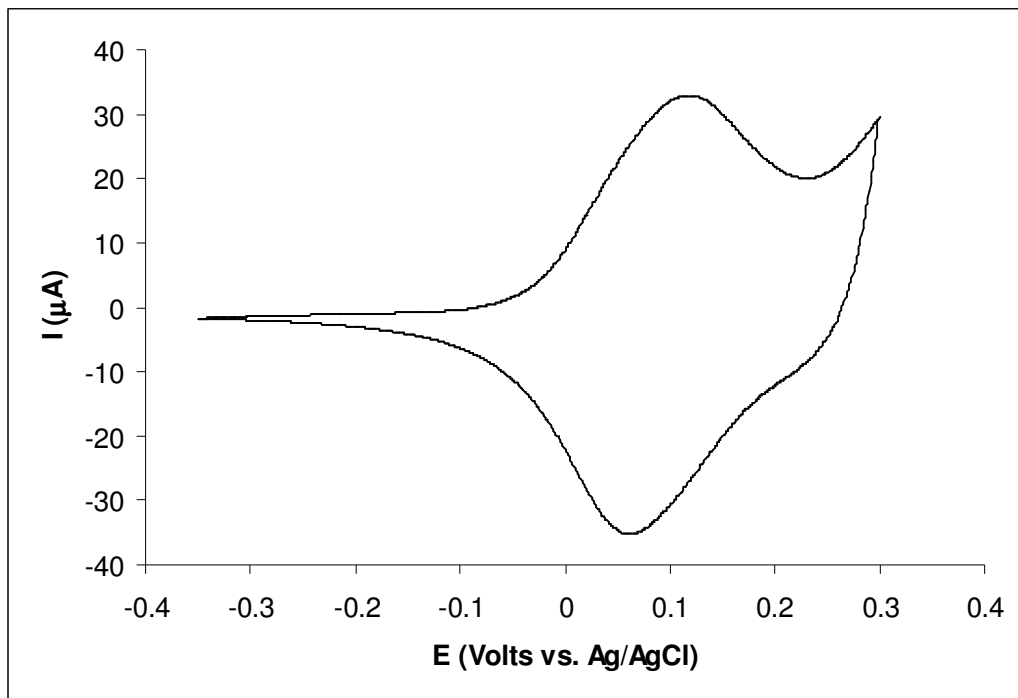


Figure 2(a)

Figure 2(b)

Figure 2(c)

Figure 2(d)

Figure 2(e)

Figure 3(a)

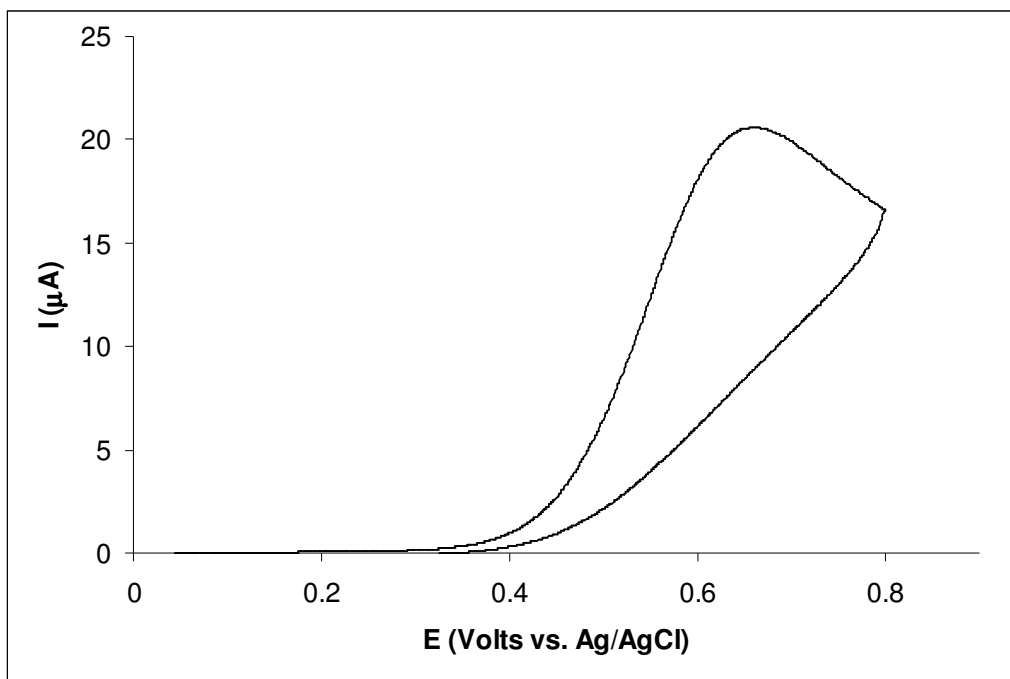


Figure 3(b)

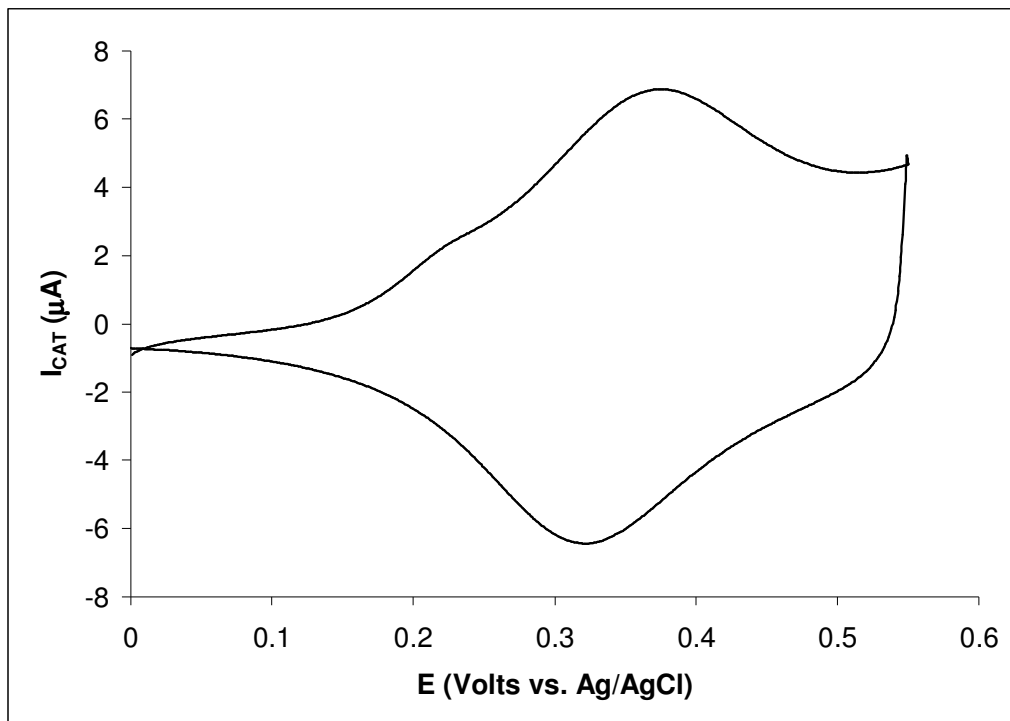


Figure 3(c)

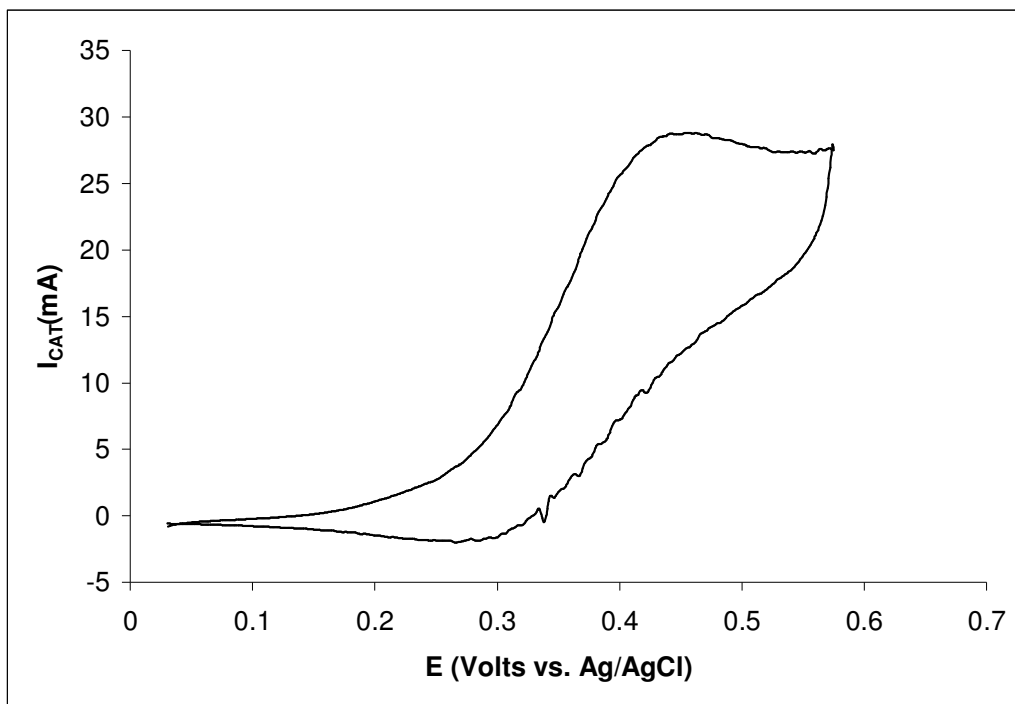


Figure 3(d)

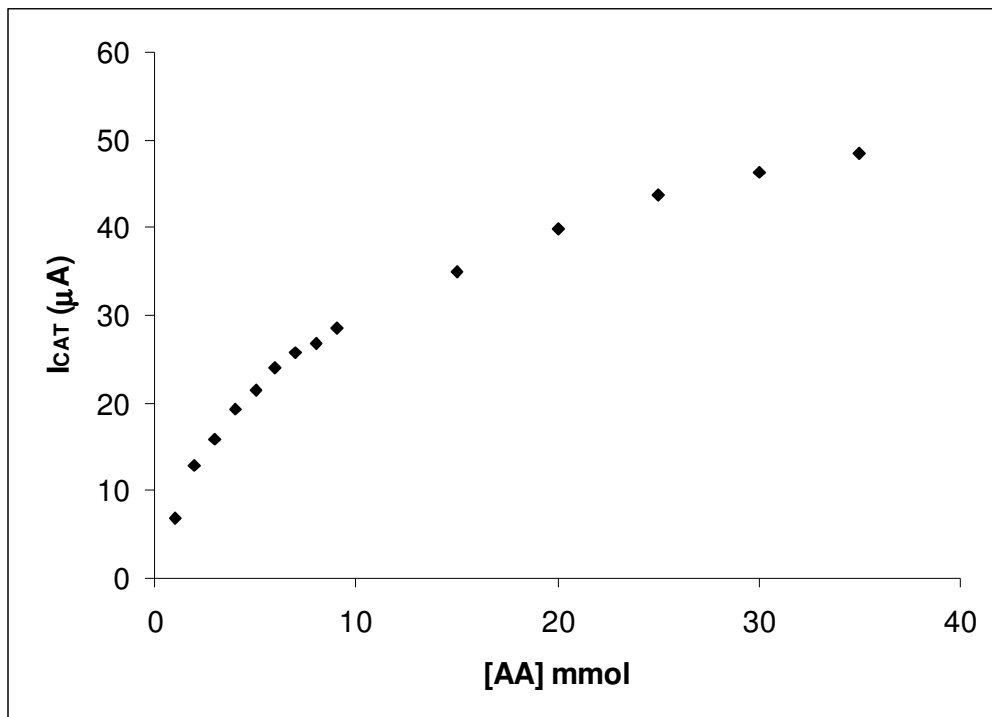


Figure 3(e)

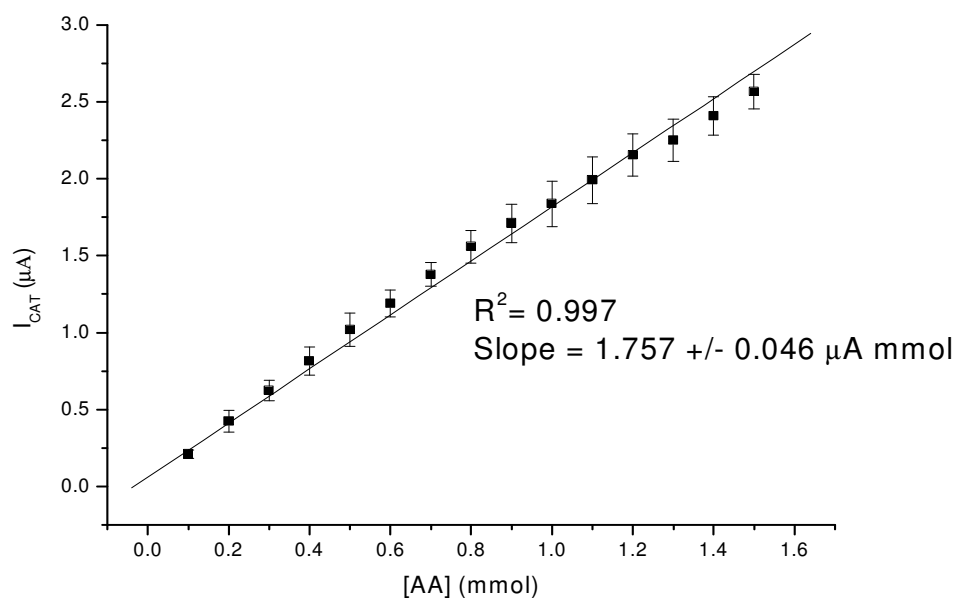


Figure 3(f)

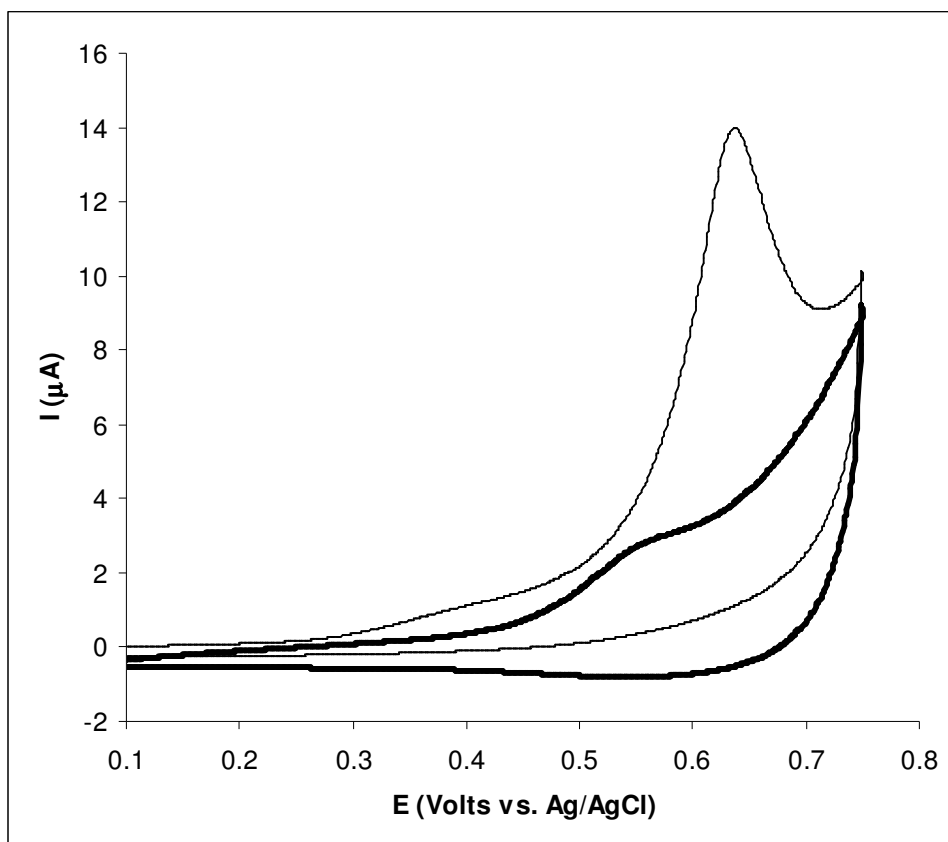


Figure 4(a)

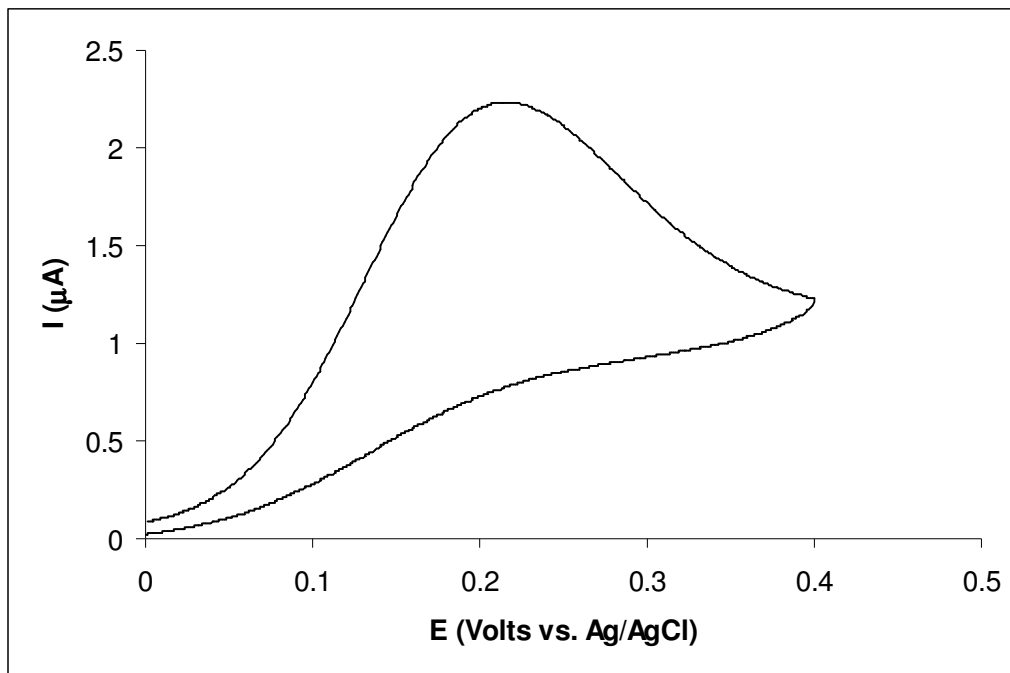


Figure 4(b)

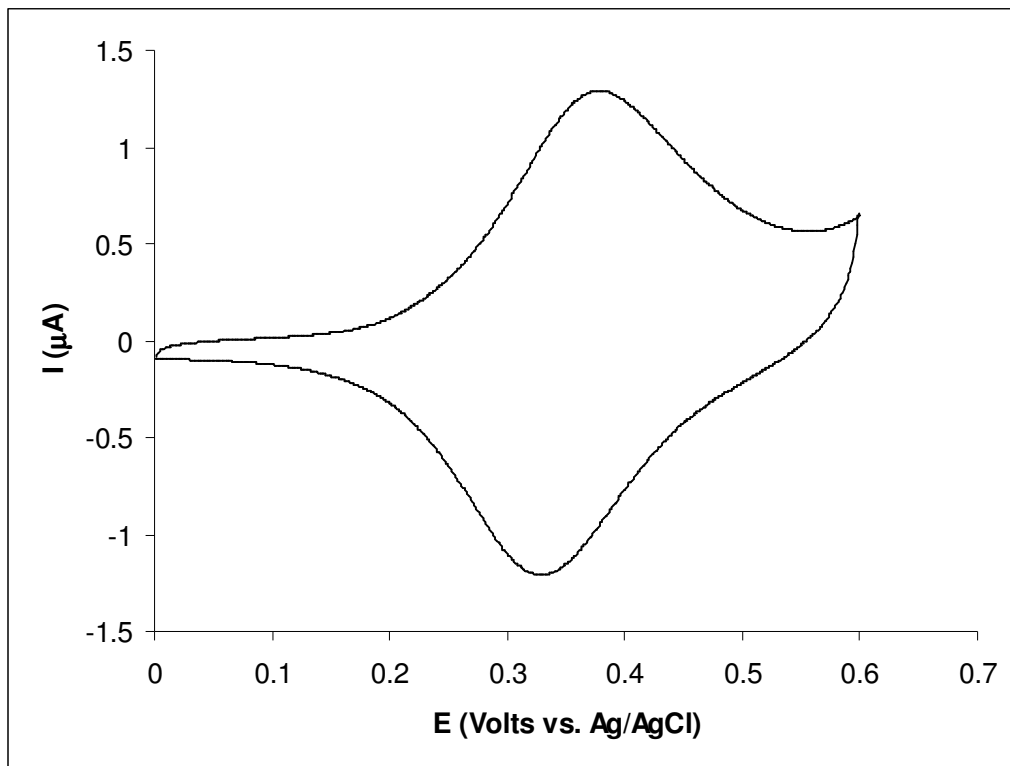


Figure 4(c)

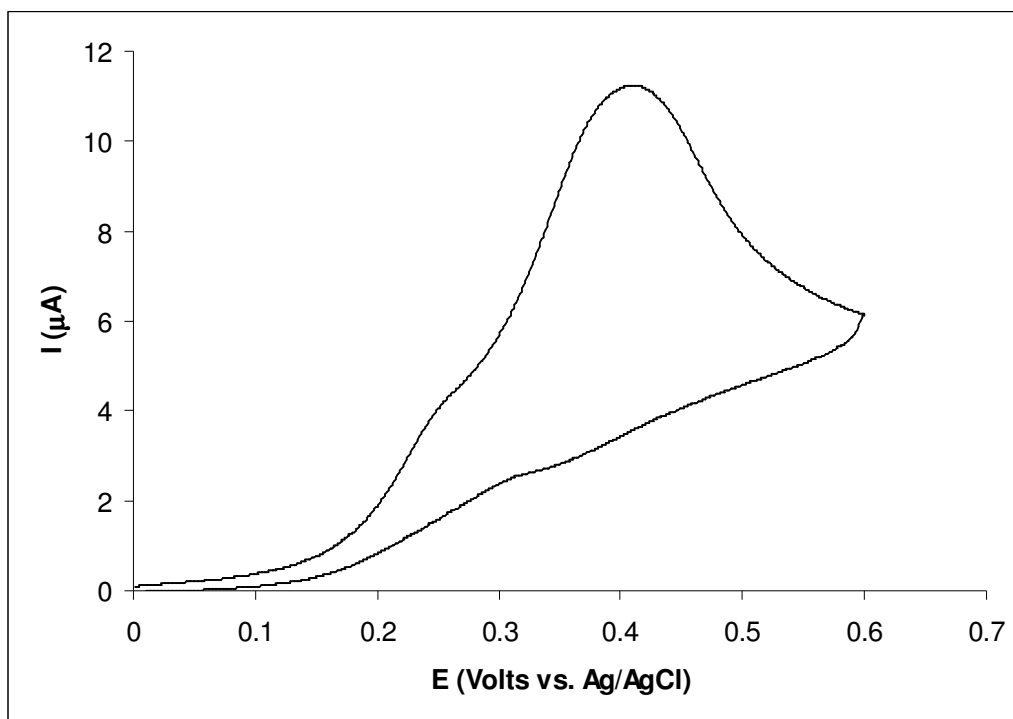


Figure 4(d)

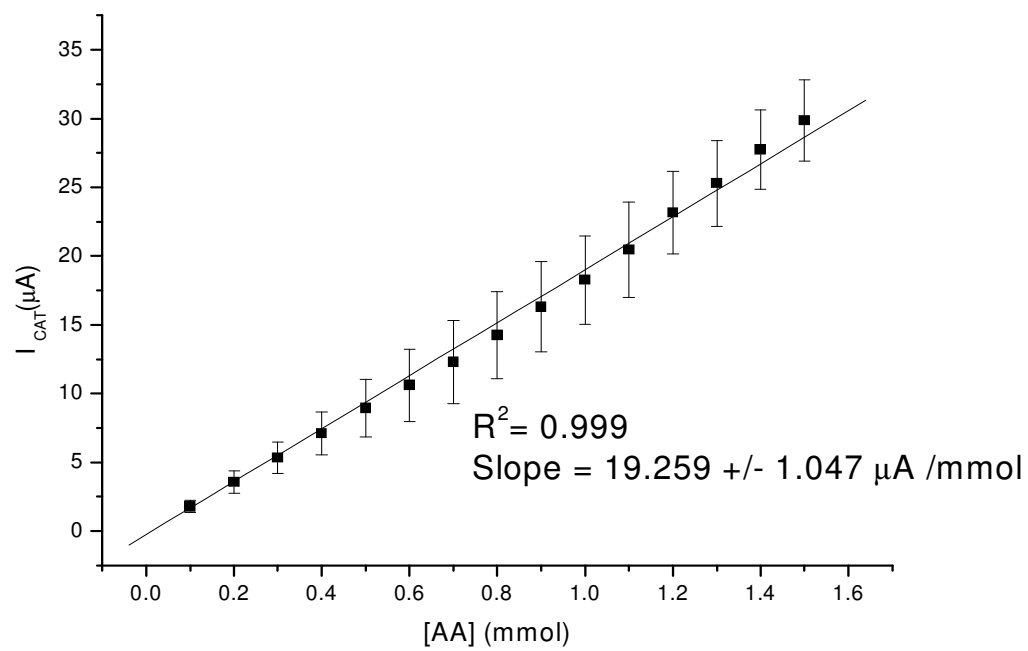


Figure 5

